

PCCP

Accepted Manuscript



This is an *Accepted Manuscript*, which has been through the Royal Society of Chemistry peer review process and has been accepted for publication.

Accepted Manuscripts are published online shortly after acceptance, before technical editing, formatting and proof reading. Using this free service, authors can make their results available to the community, in citable form, before we publish the edited article. We will replace this *Accepted Manuscript* with the edited and formatted *Advance Article* as soon as it is available.

You can find more information about *Accepted Manuscripts* in the [Information for Authors](#).

Please note that technical editing may introduce minor changes to the text and/or graphics, which may alter content. The journal's standard [Terms & Conditions](#) and the [Ethical guidelines](#) still apply. In no event shall the Royal Society of Chemistry be held responsible for any errors or omissions in this *Accepted Manuscript* or any consequences arising from the use of any information it contains.

Pnicogen and hydrogen bonds: complexes between PH_3X^+ and PH_2X systems

Ibon Alkorta,* José Elguero
Instituto de Química Médica (CSIC)
Juan de la Cierva, 3. 28006 Madrid, Spain

Sławomir J. Grabowski*
Kimika Fakultatea, Euskal Herriko Unibertsitatea UPV/EHU,
and Donostia International Physics Center (DIPC),
P.K. 1072, 20080 Donostia, Euskadi (Spain)
IKERBASQUE, Basque Foundation for Science
48011 Bilbao (Spain)

Abstract

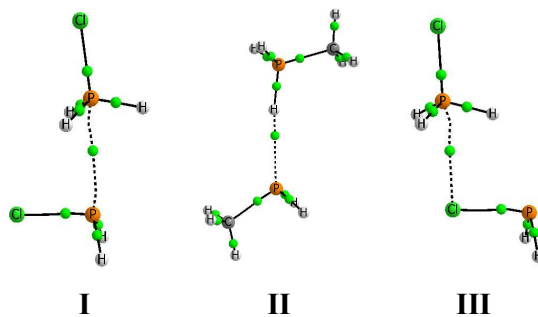
The charge-assisted complexes between PH_3X^+ and PH_2X have been analyzed. MP2/aug'-cc-pVTZ calculations were performed and the results were supported by the Quantum Theory of Atoms in Molecules approach and the Natural Bond Orbitals method. It was found that three different configurations could be formed, i.e. those linked through $\text{P}\cdots\text{P}$ or $\text{P}\cdots\text{X}$ pnicogen bond and those linked through a $\text{P-H}\cdots\text{P}$ hydrogen bond. The $\text{P}\cdots\text{P}$ configurations are the most stable ones corresponding to the strongest interactions; for all complexes the $\text{P}\cdots\text{P}$ configuration exist, while the $\text{P}\cdots\text{X}$ and $\text{P-H}\cdots\text{P}$ ones are present only for some of them. Different relations between the parameters were found, especially for the $\text{P}\cdots\text{P}$ interactions where there are correlations between the $\text{P}\cdots\text{P}$ distance and the electron density at $\text{P}\cdots\text{P}$ bond critical point (ρ_{PP}) as well as between ρ_{PP} and the charge transfer energy.

* Authors to whom correspondence should be addressed:

ibon@iqm.csic.es (IA); s.grabowski@ikerbasque.org (SJB)

Table of Contents entry

Graphic



Text

The charge-assisted complexes between PH_3X^+ and PH_2X show three potential minima structures being the pnictogen bonded (**I**) one the most stable.

Introduction

There are numerous studies on hydrogen bonds due to their role in chemistry and biology, especially in proton transfer reactions, crystal engineering and various life processes.^{1,2,3,4,5} Similarly, the role of other non-covalent interactions has also been analyzed.^{6,7,8} Amongst such interactions are the halogen,^{9,10,11,12} chalcogen,^{13,14,15} pnictogen,^{16,17,18,19,20,21,22} and tetrel^{23,24,25,26,27,28,29,30} bonds, where atoms from the 17th to the 14th group of the periodic table act as Lewis acid centers. This is surprising since these atomic centers are usually classified as electronegative. However, it should be considered that their atomic surfaces are characterized by negative and positive electrostatic potential regions; the positive regions implying Lewis acid properties.^{31,32,33,34} It was proposed that these interactions should be named σ -hole bonds, since the region of the positive electrostatic potential corresponds to a σ -hole, i.e. to the depletion of the electron charge density on the extension of one of the covalent bonds to the atom playing the role of the Lewis acid center.^{35,36,37,38,39}

In this study we deal with the pnictogen bond which has been recognized as a new and important type of intermolecular interaction.^{40,41,42,43,44,45,46,47,48,49,50,51,52,53,54,55,56,57,58,59} A pnictogen bond is the one in which the pnictogen centre (N, P, As, Sb) acting as the Lewis acid interacts with a Lewis base. There are experimental and theoretical evidences of the existence of this kind of interaction. In one of the first studies on this topic, the interactions in the crystal structures of three phosphanyl derivatives were analyzed and short N \cdots P intramolecular distances were detected and attributed to weak N \rightarrow P dative bonds.¹⁷ A short intramolecular P \cdots P distance found in the crystal structure of 1,2-(diphenylphosphino)-1,2-dicarba-*closo*-dodecaborane¹⁶ was confirmed to be attractive using B3LYP/6-31G(d) calculations and NBO analysis (P lone pair \rightarrow σ_{PC}^* donor-acceptor stabilizing interaction). Hey-Hawkins and coworkers have also analyzed pnictogen bonds⁴⁰ and they claimed that these interactions have a comparable strength to hydrogen bonds and should be considered as a new molecular linker. Furthermore, single electron pnictogen bonds were analyzed theoretically by means of MP2 and CCSD(T) methods in complexes of monosubstituted phosphines (XH₂P) and the methyl radical.⁶⁰ Two configurations corresponding to energetic minima were found for each XH₂P-CH₃ complex; the first one is characterized by short P \cdots C distances and large interactions energies, while the second one has long P \cdots C distances and weak interactions typical for the other kind of pnictogen bonded complexes, with interaction energies between -9.8 and -3.7 kJ \cdot mol⁻¹.

Different theoretical methods were applied to analyze pnictogen bonds; the ab initio calculations are often performed and supported by the analysis of the molecular electrostatic potentials, the Natural Bond Orbitals (NBO) method^{61,62} as well as the Quantum Theory of 'Atoms in Molecules' (QTAIM) approach.^{63,64,65} Recently, the possibility of using the Laplacian of the electron density to better understand the nature of pnictogen bond was described.⁶⁶ These authors used the distribution of the Laplacian of the electron density to investigate P···P, P···N and N···N pnictogen bonds showing that for these interactions a region of charge depletion and excess of kinetic energy (hole) of the pnictogen atom combines with a region of charge concentration and excess of potential energy (lump) of another species. Thus, the pnictogen bonds may be described in terms of lump-hole interactions.

Important also are the reports by Scheiner who compared such Lewis acid–Lewis base interactions as the pnictogen, chalcogen, halogen and hydrogen bonds.^{67,68} He has pointed out that although these interactions are of comparable strength, they are reinforced by the presence of an electronegative substituent on the Lewis acid centre and also they are reinforced as we move down the appropriate column of the periodic table, for example, from Cl to Br and I in the case of halogen bonds. Similar relationships connected with the increase of the atomic number have been found for pnictogen and chalcogen bonds. The latter findings are in agreement with the earlier studies of Politzer et al. who have justified that such an increase of the strength of interaction accompanying the increase of the atomic number of the Lewis acid centre in the same group of the periodic system is a result of the increase of the σ -hole and, consequently, of the positive electrostatic potential of this centre.^{18,35,36,37}

The ability of ZH_4^+ , ZH_3F^+ and ZF_4^+ cations ($Z = N, P$ or As) to form hydrogen bonds or pnictogen bonds with hydrogen cyanide and its lithium derivative was analyzed.^{69,70} It was found that for the NH_4^+ ion the N–H···N hydrogen bond is formed while for the heavier Z -centers or the ZFH_3^+ fluorinated ions, Z ···N σ -hole (or pnictogen) bonds are formed. However for some cations two configurations are possible; one linked through the hydrogen bond and the second one through the Z ···N pnictogen bond.

In the present article, complexes formed by protonation of $(PH_2X)_2$ dimers have been studied. The characteristics of these complexes have been compared with the corresponding neutral ones. There are at least two reasons to analyze such complexes: i) the protonated dimers may be linked through the pnictogen bond as well as through the

hydrogen bond; ii) one can expect stronger interactions for the protonated dimers than for the neutral analogues since it was described in the former studies that the interactions, especially hydrogen bonds, are strengthened by charge assistance.^{71,72,73} As could be expected by the Coulomb's Law the electrostatic interaction energy increases for charge assisted complexes in comparison with the neutral analogues, however the other attractive terms increase simultaneously.^{37,73}

1. Computational Methods

The calculations were carried out with the Gaussian09 set of codes⁷⁴ using the second-order Møller-Plesset perturbation theory (MP2),⁷⁵ and the aug'-cc-pVTZ basis set.⁷⁶ This basis set is composed by the Dunning aug-cc-pVTZ bases for the heavy atoms and the cc-pVTZ one for H-atoms. Frequency calculations have been carried out at the same computational level to confirm that the obtained structures correspond to energetic minima. The binding energies were calculated as differences between the energy of the complex and the sum of energies of the isolated monomers in their minima configuration thus the deformation energy being the effect of complexation process is included. The inherent Basis Set Superposition Error (BSSE) has been estimated with the counterpoise method⁷⁷ and added to the uncorrected binding energy.

The Quantum Theory of 'Atoms in Molecules' (QTAIM)^{63,64,65} was also applied to analyze critical points (BCPs) in terms of the electron density (ρ_{BCP}), its Laplacian ($\nabla^2\rho_{\text{BCP}}$) and the total electron energy density at BCP (H_{BCP}); the latter may be decomposed into the potential electron energy density (V_{BCP}) and the kinetic electron energy density (G_{BCP}). The QTAIM calculations were performed with the use of the AIMAll program.⁷⁸

The Electrostatic potentials of the isolated monomers have been calculated with the Gaussian-09 and analyze with the WFA-SAS program⁷⁹ on the 0.001 au electron density isosurface to locate the position and value of the critical points (minima and maxima).

The Natural Bond Orbital (NBO) method^{61,62} was applied to analyze orbital-orbital interactions. The $n(\text{B}) \rightarrow \sigma_{\text{AH}}^*$ overlap is often considered as the characteristic interaction of the A-H \cdots B hydrogen bond.^{61,62,80} $n(\text{B})$ designates the lone electron pair of the B proton acceptor (the Lewis base) and σ_{AH}^* is an antibonding orbital of the proton donating bond (the Lewis acid). The $n(\text{B}) \rightarrow \sigma_{\text{AH}}^*$ interaction is calculated as the second-order perturbation theory energy and, in the case of P-H \cdots P hydrogen bonds, it

corresponds to the $n(\text{P}) \rightarrow \sigma_{\text{PH}}^*$ overlap. In the same way, the pnictogen interaction can be assigned to the $n(\text{P}/\text{X}) \rightarrow \sigma_{\text{PX}}^*$ charge transfer, between a Lewis base P or X lone pair and an antibonding orbital of the PX Lewis acid, σ_{PX}^* . The NBO orbital-orbital energies were calculated at HF/aug'-cc-pVTZ level for the previously optimized geometries (MP2/aug'-cc-pVTZ level).

The NEDA decomposition scheme of the interaction energy is often applied to analyze intermolecular interactions.^{81,82,83} Correlation effects are neglected within the last approach since the decomposition is performed on the Hartree-Fock wave function. This is why an extended DFT/NEDA approach⁸⁴ is applied here to include the correlation effects. For the DFT/NEDA decomposition analysis the B3LYP functional⁸⁵ and the cc-pVTZ basis set⁸⁶ were used here for the geometries optimized earlier at MP2/aug'-cc-pVTZ level. The interaction energy within DFT/NEDA method may be expressed in the following way.

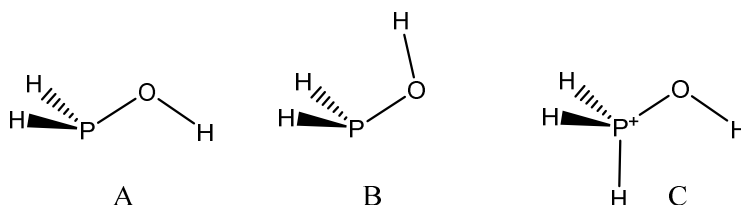
$$\text{TOT} = \text{ES} + \text{POL} + \text{CT} + \text{XC} + \text{DEF} \quad (1)$$

For a complex composed of A and B systems, TOT is the DFT total interaction energy, ES is the classical electrostatic interaction. POL, polarization term, arises from the extra electrostatic interaction connected with the polarization of the unperturbed molecular orbitals of the separated A and B fragments to those of the complex. CT, the charge transfer contribution, is the stabilizing component which arises from the delocalization of the electrons between A and B units of the complex. The XC is an attractive contribution accounting for intermolecular electron exchange and correlation. DEF is the deformation energy having a contribution from each fragment, DEF(A) and DEF(B). DEF(A or B) is a repulsive term since $\psi_{\text{A(B)}}$, the wave function converged for A(B), is of lower energy than $\psi_{\text{A(B)}}^{\text{def}}$ in the complex. The DFT/NEDA decomposition has been chosen here because the extended basis sets calculations have shown the numerical stability of this approach.⁸⁴ For the Natural Bond Orbital (NBO) and DFT/NEDA calculations the NBO 5.0 program⁸⁷ implemented in the GAMESS set of codes⁸⁸ was used.

2. Results and Discussions

3.1 Protonated phosphines

Initially, the stability of the cations resulting of the protonation on the different sites of the PH_2X phosphines, with $\text{X} = \text{H}, \text{F}, \text{OH}, \text{NH}_2, \text{NC}, \text{CH}_3, \text{CN}, \text{CCH},$ and Cl , has been analyzed. Two conformers of the H_2POH molecule, A and B (Scheme 1) have been examined but in both cases, the protonation leads to the same cation C (Scheme 1). For the neutral species, conformation A is more stable than conformation B by $1.3 \text{ kJ}\cdot\text{mol}^{-1}$.



Scheme 1. The two minima of the hydroxyphosphine (A and B) and the protonated form (C).

It was found that for the $\text{X} = \text{H}, \text{F}, \text{OH}, \text{CCH}, \text{CH}_3$ and Cl substituents, the most stable protonated system corresponds to that with the hydrogen atom attached to the phosphorus atom while in the case of $\text{X} = \text{NH}_2, \text{CN}$ and NC the protonation on the X groups provide more stable cations (see Table 1). Since our interest is the study of systems protonated on the phosphorous atom, the latter set of X substituents is not considered here any more. The experimental proton affinities (PA) are available only for the PH_3 and PH_2CH_3 molecules. In both cases, the differences between calculated and experimental results do not exceed $2 \text{ kJ}\cdot\text{mol}^{-1}$ (Table 1). This agreement between experimental and theoretical results show that the choice of the MP2/aug'-cc-pVTZ level to further analyze the protonated dimer phosphines, $\text{PH}_3\text{X}^+:\text{PH}_2\text{X}$, is the proper one.

Table 1. Proton affinity and relative energy ($\text{kJ}\cdot\text{mol}^{-1}$) of the different protonated species. Experimental values in parenthesis.⁸⁹ The P and X columns correspond to the protonation at the P and X centers. The last column (ΔE) is the difference between P and X proton affinities.

Substituent	Protonation site		Difference
	P	X	
X			ΔE^*
F	767.4	595.2	178.3

Cl	769.8	642.6	134.9
OH	820.0	731.1	87.3
NC	725.6	836.8	-112.1
NH ₂	849.1	854.7	-14.4
CCH	802.3	745.7	56.6
CN	707.1	766.5	-60.6
CH ₃	852.8 (851.5)	-	
H	783.8 (785)	-	

* Positive values indicate that the protonation on the phosphorus atoms is more favorable than on the X group.

Table 2. The maxima of the electrostatic potential (in au) on the 0.001 au electron density isosurfaces of PH₃X⁺ units. The location of maxima corresponds to the σ -holes associated to the X-P bond (in the case of PH₄⁺ it is an H-P bond).

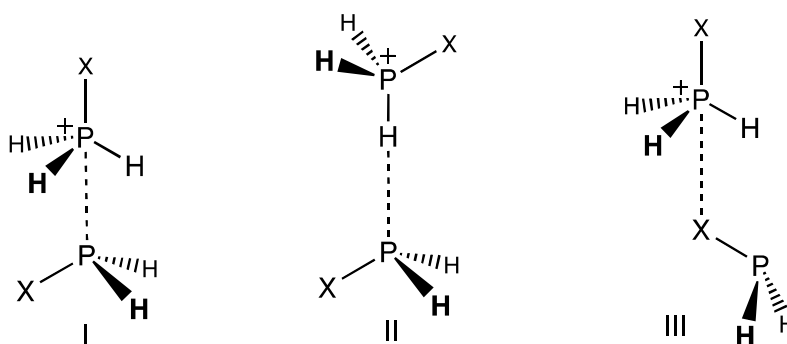
Cation	σ -hole
PH ₃ F ⁺	0.313
PH ₃ Cl ⁺	0.278
PH ₂ OH ⁺	0.282
PH ₃ CCH ⁺	0.259
PH ₃ CH ₃ ⁺	0.243
PH ₄ ⁺	0.268

The maximum positive electrostatic potential values on the P-centre for PH₄⁺ and its derivatives are listed in Table 2. In all cases, the positive region associated with the elongation of H-P bond shows less positive value than the σ -hole region associated with the elongation of the X-P bond. One can expect the strongest acidic properties of the phosphorus centre for the PH₃F⁺ cation complexes and the weakest ones for the PH₃CH₃⁺ cation complexes based on the electrostatic potential values. It is interesting that for all cations listed in Table 2, the phosphorus atom is a stronger Lewis acid centre than the attached hydrogen atoms since a greater electrostatic potential is detected for the P-centre than for H-atoms. It suggests preferences to form P \cdots P pnictogen bonds than to form P-H \cdots P hydrogen bonds in the PH₃X⁺-PH₂X systems.

3.2 PH₃X⁺:PH₂X complexes – geometry and energy

Initially, two types of complexes have been tested: those with a P \cdots P interaction (**I** in Scheme 2) and those linked through a P-H \cdots P hydrogen bond (**II** in Scheme 2). In all cases, the complexes with P \cdots P interaction correspond to local minima. However, only

in three cases hydrogen bonded complexes have been located, those for $X = H$, CH_3 and $OH-A$; in the remaining cases ($X = F$, Cl , $OH-B$ and CCH), the optimization evolves towards a pnictogen bonded complex with a $P \cdots X$ interaction (**III** in Scheme 2). However, in few cases of configuration **III**, the $P \cdots X$ pnictogen bond can be accompanied by additional $P-H \cdots P$ hydrogen bond interactions. This will be discussed later on. The formation of the $P \cdots P$ pnictogen bonds for all cations is, at least, partly a consequence of the most positive electrostatic potential associated to the P-atom (Table 2); for the less positive potential of the H-atoms, only in few cases the hydrogen bond is formed, as was discussed in the previous section.



Scheme 2. Configurations **I-III**.

There is not a single complex where all three configurations exist. For example, attempts to locate the hydrogen bonded configuration corresponding to an energy minimum for the $PH_3F^+ : PH_2F$ complex always led to the minima corresponding to configurations **I** and **III**. Figure 1 presents examples of configurations mentioned above, i.e. linked through $P \cdots P$ (**I**), $P-H \cdots P$ (**II**) and $X \cdots P$ (**III**) interactions.

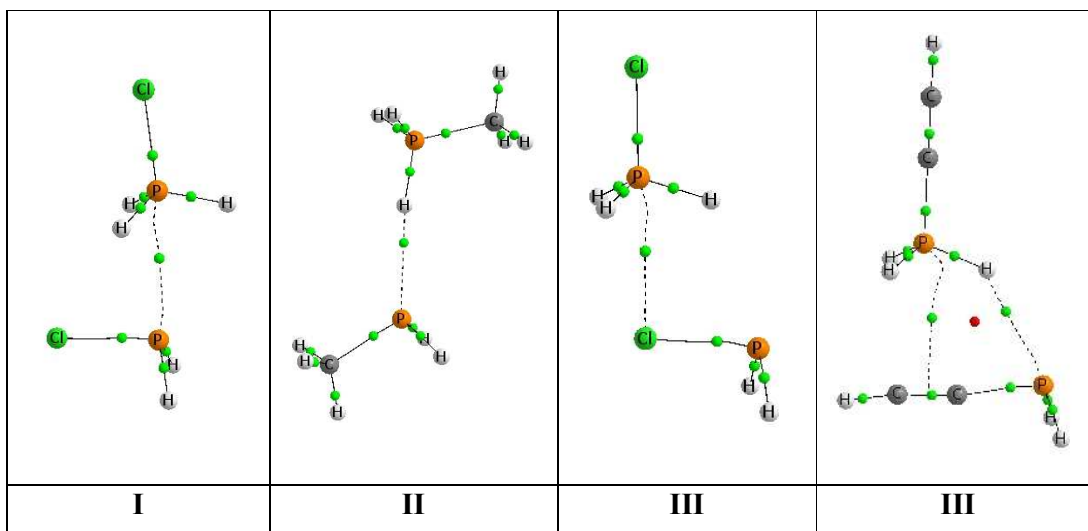


Fig. 1 Molecular graphs of selected $\text{PH}_3\text{X}^+:\text{PH}_2\text{X}$ complexes; examples for the three configurations are presented.

It is interesting that in the case of configuration **I**, for $\text{X} = \text{H}$ and CH_3 , the substituents in the P atoms are eclipsed while in the remaining configurations linked by the $\text{P}\cdots\text{P}$ interaction they are alternated. The $\text{PH}_3\text{CCH}^+:\text{PH}_2\text{CCH}$ complex is an interesting case since two configurations were found to correspond to energetic minima, i.e. the pnictogen bonded complex linked through the $\text{P}\cdots\text{P}$ interaction (**I**) and the complex attributed earlier here to the configuration **III**. However, in the latter case two links are observed, the link corresponding to the $\text{P}-\text{H}\cdots\text{P}$ hydrogen bond analogous to those of configuration **II** and the pnictogen bond between the P-centre of PH_3CCH^+ and π -electrons of the acetylene substituent in the PH_2CCH moiety. The molecular graph of this structure is shown on the right side of Fig. 1 and one can see bond paths with bond critical points (BCPs) corresponding to the links described above, $\text{H}\cdots\text{P}$ and $\text{P}\cdots\pi$ (π corresponds here to the BCP of the $\text{C}\equiv\text{C}$ bond of the acetylene substituent). Note that there are additional structures corresponding to local minima associated to the Configurations **I**, **II** and **III** presented in Scheme 2. However these structures are less stable (they are characterized by higher energies) than those chosen and analyzed here. The complexes analyzed in this study resemble to those between $\text{X}=\text{PH}_3$ and phosphorus and nitrogen bases published by some of us.⁹⁰

Table 3. Interatomic distance (Å) of the $\text{PH}_3\text{X}^+:\text{PH}_2\text{X}$ complexes.

Substituent	I (P···P)	II (P···H)	III
F	2.698		2.362 (P···F)
Cl	3.050		2.957 (P···Cl)
OH-A	2.963	2.516	
OH-B	2.941		2.446 (P···O)
CCH	3.249		2.650 (P···H) 3.150 (P···C)
CH ₃	3.368	2.495	
H	3.356	2.456	

Table 3 presents the interatomic distances in the $\text{PH}_3\text{X}^+:\text{PH}_2\text{X}$ complexes. The P···P distances in configuration **I** range from 2.70 to 3.37 Å being shorter in the fluorine complex while the longest corresponds to the methyl derivatives complex. The three minima found with configuration **II** have P···H distances around 2.5 Å. Finally, the intermolecular distances in the complexes in configuration **III** are very variable since they correspond to the interaction of the phosphorous with a variety of atoms (F, Cl, O and C).

Table 4 presents the uncorrected and BSSE corrected binding energies for all configurations corresponding to energetic minima, the binding energies for the neutral dimers are also included for comparison. The BSSE correction ranges between 7 and 3% of the uncorrected value at MP2/aug'-cc-pVTZ. However, care should be taken for the corrected E_b values since those values for the $\text{PH}_4^+:\text{PH}_3$ complex show larger error than the uncorrected ones when compared to the MP2/aug'-cc-pVQZ and MP2/aug'-cc-pV5Z results. These results are in agreement with recent reports that indicate that the corrected E_b could provide a larger error than the uncorrected ones.^{91, 92}

Table 4. Uncorrected and BSSE corrected binding energies ($\text{kJ}\cdot\text{mol}^{-1}$) of the different minima located in the PES at the MP2/aug'-cc-pVTZ computational level. For the $\text{PH}_4^+:\text{PH}_3$ complex, the calculations with the MP2/aug'-cc-pVQZ and MP2/aug'-cc-pV5Z computational level are also indicated.

X	Uncorrected E_b			BSSE corrected E_b		
	I	II	III	I	II	III
F	-74.9		-70.8	-70.2		-66.8
Cl	-55.4		-59.3	-51.5		-55.6
OH-A	-57.9	-30.2		-54.6	-28.8	
OH-B	-77.1		-81.2	-73.6		-77.3
CCH	-55.2		-54.9	-51.6		-51.0

CH ₃	-52.1	-43.8		-50.0	-42.4	
H	-46.1	-38.8		-44.4	-37.6	
H (MP2/aug'-cc-pVQZ)	-47.0	-39.1		-46.3	-38.5	
H (MP2/aug'-cc-pV5Z)	-47.5	-39.0		-47.2	-38.7	

Configuration **I**, characterized by the P...P interaction, is more stable in all complexes than configuration **II** where there is a P-H...P link. There are four configurations characterized by P...X interactions (**III**). In the cases of X = F and CCH substituents, **I** with P...P interactions is more stable than that with P...X links (**III**), in the two remaining cases (X = OH-B and Cl) both configurations are energetically very close to each other (see Table 4). Table 4 shows that the strongest P...P and P...X interactions occur for the PH₃F⁺:PH₂F and PH₃OH⁺:PH₂OH complexes, respectively. The latter complexes with the OH substituent are characterized by the conformation B of the PH₃OH neutral moiety (see Scheme 1) acting as the Lewis base. The interactions in the PH₃OH⁺:PH₂OH complexes with the A conformer of the Lewis base are characterized by weaker interactions than those of the B conformer.

The binding energy in complexes in configuration **I** does not follow the ranking expected based on the values of the σ -hole of the isolated monomers described in the previous section. Thus, the PH₄⁺:PH₃ complex is the weakest one while the σ -hole of PH₄⁺ is larger than those with X = CH₃ and CCH. However, the different stability of the two complexes with X=OH can be explain based on the larger value of the electrostatic potential minima associated to the lone pair of the neutral molecule in conformation B (-0.030 au.) vs. the one in conformation A (-0.024 au).⁹³

On the other hand, we have found that the group electronegativity of X [F(3.98), Cl(3.16), OH(3.51), CCH(2.90), CH₃(2.27) and H(2.20)]^{94, 95} follows the same order as the binding energies. Thus, it is clear that to predict the binding energy, the electronegativity that provides a more general idea of the electronic effect of an atom or a chemical group is a better descriptor than the σ -hole value, a property in a single special point of the isolated molecule. Other factors as the polarization can modulate these results.³⁹

3.3 PH₃X⁺:PH₂X complexes – QTAIM parameters and NBO

Fig. 1 shows the molecular graphs derived from the analysis of the electron density of some of the complexes (the molecular graphs of all the complexes are reported in Table S1 of the Supporting Information material). Table 5 presents the characteristics of the

bond critical point (BCP) situated on the bond path corresponding to the P \cdots P, P-H \cdots P and X \cdots P interactions.

The topological analysis of the complexes **I** present a single intermolecular BCP connecting the two phosphorous atoms. The electron density at BCP, ρ_{BCP} , is often used as a descriptor of the strength of the corresponding interaction,^{80,96,97} however here the linear correlation between the binding energy and the electron density at P \cdots P BCP (ρ_{PP}) is poor, providing a $R^2 = 0.64$. On the other hand, the electron density at BCP often correlates with the distance between the interacting centers.^{98,99,100,101} Figure 2 shows the exponential relationship between the P \cdots P distance and ρ_{PP} . It has been explained that such dependence reflects the nature of interactions which exactly change exponentially with the change of the distance.^{102,103} For small ranges of interatomic distances a linear distance- ρ_{BCP} dependence is often found.

Table 5. QTAIM parameters (in au) for the BCPs corresponding to the P \cdots P, P-H \cdots P and P \cdots X interactions, the electron density at BCP, ρ_{BCP} , its Laplacian, $\nabla^2\rho_{\text{BCP}}$, the total electron energy density at BCP, H_{BCP} , and the components of the latter value, the kinetic, G_{BCP} , and potential, V_{BCP} , energies.

X	ρ_{BCP}	$\nabla^2\rho_{\text{BCP}}$	G_{BCP}	V_{BCP}	H_{BCP}
I (P\cdotsP)					
F	0.0475	0.0140	0.0177	-0.0319	-0.0142
Cl	0.0228	0.0386	0.0118	-0.0140	-0.0022
OH-A	0.0291	0.0358	0.0135	-0.0180	-0.0045
OH-B	0.0282	0.0394	0.0140	-0.0181	-0.0041
CCH	0.0151	0.0349	0.0089	-0.0090	-0.0002
CH ₃	0.0141	0.0308	0.0077	-0.0078	0.0000
H	0.0139	0.0295	0.0074	-0.0075	-0.0001
II (P\cdotsH)					
OH-A	0.0213	0.0327	0.0094	-0.0106	-0.0012
CH ₃	0.0219	0.0335	0.0097	-0.0112	-0.0014
H	0.0229	0.0337	0.0101	-0.0118	-0.0018
III					
F (P \cdots F)	0.0290	0.1008	0.0263	-0.0274	-0.0012
Cl (P \cdots Cl)	0.0206	0.0512	0.0136	-0.0144	-0.0008
OH-B (P \cdots O)	0.0304	0.0894	0.0243	-0.0262	-0.0019
CCH (P \cdots H)	0.0136	0.0335	0.0078	-0.0072	0.0006
CCH (P \cdots π)	0.0125	0.0360	0.0081	-0.0073	0.0008

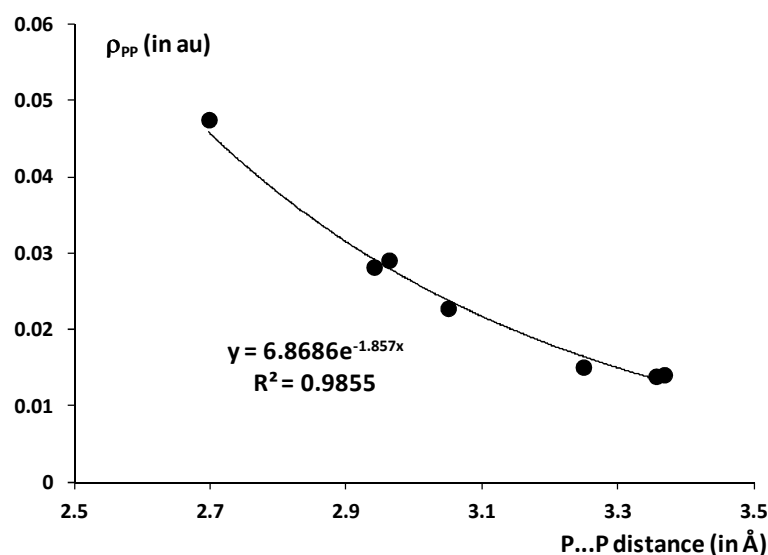


Fig 2. The relationship between the P...P distance and the electron density at the corresponding BCP.

It has been stated that the negative value of the total electron energy density at BCP, H_{BCP} , confirms the covalent character of the corresponding interaction.^{104,105,106} This was particularly studied for hydrogen bonds and justified that the hydrogen bonds characterized by a negative H_{BCP} were classified as the strong interactions possessing some covalent character.^{80,97} Table 5 shows negative values of the total electron energy density at P...P BCP, H_{PP} , for more electronegative substituents while for CH_3 , H and CCH the H_{PP} value is close to zero. One can also see that the most negative values of H_{PP} correspond to the stronger interactions (see binding energies in Table 4) and to the greater values of ρ_{PP} (Table 5).

Four H...P hydrogen bonds BCP are found in the studied complexes, they correspond to the complexes in configuration **II** and the P-H...P interaction observed in the $PH_3CCH^+ : PH_2CCH$ complex, configuration **III**. ρ_{BCP} ranges between 0.014 and 0.023 au, being as usual their values larger as the interatomic distances are shorter. All of them present positive values of the Laplacian and small and negative values of the total energy density save in the case of the BCP of the $PH_3CCH^+ : PH_2CCH$ complex that shows a small positive value of H.

The four BCPs, due to the interaction of the protonated phosphine with the X group in configuration III, show ρ_{BCP} values between 0.013 and 0.03 au and positive

values of the Laplacian. As in the case of intermolecular BCP of the minima in configuration **II**, small and negative values of H are obtained save for the BCP of the $\text{PH}_3\text{CCH}^+:\text{PH}_2\text{CCH}$ complex.

Table 6 presents the charge transfer for the complexes studied here. It is calculated from the QTAIM integrated charges and expresses the amount of the electron charge transferred from the neutral Lewis base unit into the positively charged Lewis acid species. The main NBO orbital-orbital interactions are also included in the Table and the corresponding values of energies are reported. Let us consider first the configurations **I** where the $\text{P}\cdots\text{P}$ interaction is the main interaction. The $n(\text{P}) \rightarrow \sigma_{\text{PH}}^*$ or $n(\text{P}) \rightarrow \sigma_{\text{PX}}^*$ orbital-orbital interaction for those species where X corresponds to the electronegative O or Cl atom or to the carbon centre in a case of CH_3 and CCH substituents is the most important one.

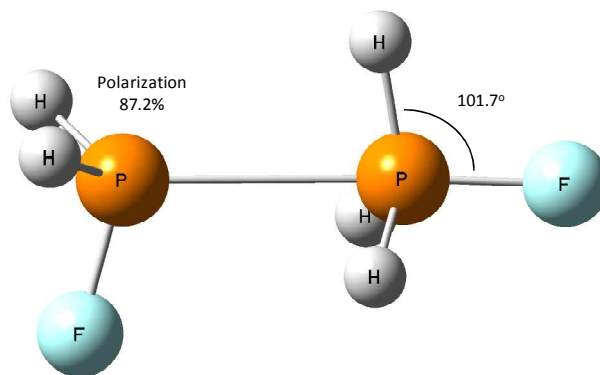
Table 6 shows that the intermolecular orbital charge transfer energies for complexes in configurations **I** and **II** are in agreement with the AIM results. However, in the case of configuration **III**, important contributions of the $\text{P-H}\cdots\text{P}$ interactions for $\text{PH}_3\text{Cl}^+:\text{PH}_2\text{Cl}$ and $\text{PH}_3\text{OH}^+:\text{PH}_2\text{OH}$ complexes are found that are not reflected by the corresponding BCP and bond path in the analysis of the electron density. In the $\text{PH}_3\text{CCH}^+:\text{PH}_2\text{CCH}$ complex (configuration **III**) both NBO and AIM indicate the stabilizing nature of the $\text{P-H}\cdots\text{P}$ interaction. The lack of an agreement for some interactions between NBO and AIM methodologies has already been described in the literature. Thus, for the $\text{H}\cdots\text{H}$ intramolecular contacts between a typical Lewis acid (OH bond) and the Lewis base (BH_2 and AlH_2) the stabilizing $\sigma_{\text{BH/AlH}} \rightarrow \sigma_{\text{OH}}^*$ energy lowering exists even if the appropriate bond path with BCP is not detected.¹⁰⁷ Similar situations were analyzed for $\text{O-H}\cdots\text{O}$ and $\text{N-H}\cdots\text{O}$ intramolecular hydrogen bonds where the NBO method shows the existence of stabilizing $n(\text{O}) \rightarrow \sigma_{\text{OH}}^*$ and $n(\text{O}) \rightarrow \sigma_{\text{NH}}^*$ orbital-orbital overlaps but the bond paths do not exist.¹⁰⁸ This may be partly rationalized in terms of the physical meaning of the bond paths which may be treated as the indicators of the preferable interactions:^{109,110,111} if the orbital-orbital overlap corresponds to the stronger interaction thus the bond path is detected (refs. ^{107,108} and results presented here).

Table 6. QTAIM electron charge shift from the Lewis base to the Lewis acid (au) and E_{NBO} orbital charge transfer energies ($\text{kJ}\cdot\text{mol}^{-1}$) - the corresponding charge donor orbital- acceptor orbital is listed.

X	Change transfer	E_{NBO}	interaction
I			
F	0.220	-	Covalent
Cl	0.111	33.1	$n(\text{P}) \rightarrow \sigma_{\text{PCl}}^*$
OH-A	0.163	52.5	$n(\text{P}) \rightarrow \sigma_{\text{PO}}^*$
OH-B	0.129	48.3	$n(\text{P}) \rightarrow \sigma_{\text{PO}}^*$
CCH	0.075	16.8	$n(\text{P}) \rightarrow \sigma_{\text{PC}}^*$
CH_3	0.070	17.3	$n(\text{P}) \rightarrow \sigma_{\text{PC}}^*$
H	0.067	17.7	$n(\text{P}) \rightarrow \sigma_{\text{PH}}^*$
II			
OH-A	0.075	60.1	$n(\text{P}) \rightarrow \sigma_{\text{PH}}^*$
CH_3	0.076	64.5	$n(\text{P}) \rightarrow \sigma_{\text{PH}}^*$
H	0.078	68.5	$n(\text{P}) \rightarrow \sigma_{\text{PH}}^*$
III			
F	0.045	30.2	$n(\text{F}) \rightarrow \sigma_{\text{PF}}^*$
Cl	0.076	32.0	$n(\text{Cl}) \rightarrow \sigma_{\text{PCl}}^*$
		5.9	$n(\text{P}) \rightarrow \sigma_{\text{PH}}^*$
OH-B	0.064	35.9	$n(\text{O}) \rightarrow \sigma_{\text{PO}}^*$
		5.3	$n(\text{P}) \rightarrow \sigma_{\text{PH}}^*$
CCH	0.076	10.5	$n(\pi) \rightarrow \sigma_{\text{PC}}^*$
		14.6	$n(\text{P}) \rightarrow \sigma_{\text{PH}}^*$

Among **I** configurations, the $\text{PH}_3\text{F}^+:\text{PH}_2\text{F}$ complex is the only one where the orbital-orbital interaction is not present, since its $\text{P}\cdots\text{P}$ interaction is classified as a covalent bond by the NBO method. The occupancy of the σ_{PP} bond amounts to 1.85 electrons for this complex and the bond polarization is equal to 87.2%. The latter value expresses the percentage of the electron density at the P-atom of the PH_2F sub-unit (see Scheme 3), initially treated as the neutral one.

One of the P atom in the $\text{PH}_3\text{F}^+:\text{PH}_2\text{F}$ complex (Scheme 3) is characterized by pentavalency, i.e. is hypervalent. This situation is similar to the one described for the intermediate in the hydration of the phosphoric acid and phosphate esters that yields pentahydroxyphosphorane derivatives, which corresponds to a P(V) atom.^{112,113}

Scheme 3. Structure of the $\text{FH}_2\text{P}\cdots\text{H}_3\text{PF}$ cation

In the case of O and Cl atoms connected with the P-atom playing the role of the Lewis acid centre, the orbital-orbital interactions are much stronger than in the case of $X = \text{H}$ or C (Table 6). This is partly related to the σ -hole, i.e. the depletion of the electron charge in the elongation of X-P or H-P bond. Note that the positive electrostatic potential at P-atom is greater for more electronegative F, Cl and OH substituents than for the remaining ones (Table 2). Also the electron charge shift from the Lewis base to the Lewis acid unit (designated as transfer in Table 6) is much greater for the mentioned above more electronegative substituents than for the remaining H, CH_3 and CCH ones. For the complexes in configuration **I**, an exponential relationship between the $\text{P}\cdots\text{P}$ distance and the electron charge transfer has been found with a correlation coefficient $R^2 = 0.97$.

On the other hand, for configurations **I**, there is an excellent linear correlation ($R^2 = 0.98$) between the energy corresponding to the $n(\text{P}) \rightarrow \sigma_{\text{PX}/\text{H}}^*$ interaction (Table 6) and ρ_{PP} (Table 5) as well as between the charge transfer (Table 6) and ρ_{PP} where the linear correlation coefficient R^2 is equal to 0.97. This means that ρ_{PP} for the systems analyzed here is a good indicator of the local atom-atom interaction ($\text{P}\cdots\text{P}$) as well as that it refers to the energies related to the electron charge shift. The latter energies are often attributed to the covalency of interaction.⁷⁸

A different situation is observed for the complexes linked through a $\text{P-H}\cdots\text{P}$ hydrogen bond. For **II** complexes, the electron charge shift amounts to ~ 0.08 au (Table 6), less than most of the cases of the $\text{P}\cdots\text{P}$ pnictogen bonds (**I**) discussed earlier. The $n(\text{P}) \rightarrow \sigma_{\text{PH}}^*$ overlap energy for this group of complexes (**II**) amounts ~ 60 $\text{kJ}\cdot\text{mol}^{-1}$,

more than the $n(\text{P}) \rightarrow \sigma_{\text{PH}(\text{Cl})}^*$ energy for all complexes linked through P...P pnictogen bond. It is worth mentioning that the $n(\text{P}) \rightarrow \sigma_{\text{PH}}^*$ overlap attributed to the hydrogen bond interaction is detected for some complexes classified as configuration **III** (Table 6). However the corresponding energy is equal here to 5.9, 5.3 and 14.6 $\text{kJ}\cdot\text{mol}^{-1}$ for Cl, OH and CCH substituents, respectively. It is much lower than for the species linked only through the hydrogen bond.

The configuration **III** corresponds formally to the X...P interaction previously mentioned. However based on the NBO analysis this is only true for the $\text{PH}_3\text{F}^+:\text{PH}_2\text{F}$ complex, where other interactions are not detected (there is only one intermolecular P...F bond path for this complex). In this case, the electron charge shift to the Lewis acid is the lowest one among the complexes classified as configurations **III** (Table 6). This is probably connected with the fact that the fluorine centre is usually classified as a hard Lewis base not sensitive to the effects of polarization. Besides, for all remaining complexes of this group (**III**) additional P-H...P links are detected with the corresponding $n(\text{P}) \rightarrow \sigma_{\text{PH}}^*$ overlap enhancing additionally the electron charge shift from the Lewis base unit to the Lewis acid.

The $n(\text{P}) \rightarrow \sigma_{\text{PX}}^*$ overlap energy for the group (**III**) is between 30-36 $\text{kJ}\cdot\text{mol}^{-1}$ except of the X = CCH substituent where such energy is much lower, of about 10 $\text{kJ}\cdot\text{mol}^{-1}$. However in the latter case, the P-H...P hydrogen bond is probably a stronger interaction than the pnictogen bond.

These results justified that the P...P and P...X pnictogen bonds attributed to configurations **I** and **III** should be classified as σ -hole bonds. It was stated earlier that also hydrogen bonds probably belong to this class of interactions.^{8,114} It was shown that for the σ -hole bonds as well as for the hydrogen bonds there is an electron charge shift for the system playing the role of the electron acceptor. However, it was shown that the nature of such shift in the case of the hydrogen bond is different than in the case of the σ -hole bonds.¹¹⁵ This is why the pnictogen and hydrogen bonds possess distinct characteristics.

3.4 $\text{PH}_3\text{X}^+:\text{PH}_2\text{X}$ complexes – DFT/NEDA decomposition of the energy of interaction

The DFT/NEDA decomposition of the interaction energies has been gathered in Table 7. For the P...P pnictogen bonded complexes (configuration **I**), the energy terms attributed to the electron charge shift (CT and POL) are attractive and more important

than the electrostatic contribution (ES). The XC term related to the other effects, among them to the correlation energy, is the less important attractive term for P...P pnictogen bonds as well as for all other interactions (P...X and P-H...P).

Table 7. DFT/NEDA decomposition results, the energy terms (in $\text{kJ}\cdot\text{mol}^{-1}$) are described in the section on computational details (eq. 3).

X	TOT	CT	ES	POL	XC	DEF
I						
F	-98.1	-324.6	-136.2	-145.7	-52.0	560.4
Cl	-48.6	-119.7	-52.5	-144.3	-33.5	301.4
OH-A	-68.4	-183.5	-94.7	-101.2	-33.6	344.5
OH-B	-79.8	-163.3	-98.4	-131.7	-35.8	349.4
CCH	-41.3	-67.7	-44.3	-103.6	-25.7	200.0
CH ₃	-46.5	-59.5	-57.1	-73.6	-17.7	161.4
H	-42.9	-55.1	-47.0	-78.6	-17.4	155.2
II						
OH-A	-34.9	-97.3	-34.9	-18.3	-13.6	129.3
CH ₃	-45.2	-89.6	-48.0	-37.0	-15.9	145.3
H	-43.0	-92.9	-41.0	-38.5	-16.6	146.1
III						
F	-73.4	-93.6	-85.2	-147.5	-36.6	289.6
Cl	-45.2	-89.6	-48.0	-37.0	-15.9	145.3
OH-B	-78.2	-114.8	-104.3	-196.2	-49.0	386.1
CCH	-40.6	-67.9	-46.5	-96.2	-27.9	197.8

It was shown in the previous sections that the electron charge transfer for P...P interactions is greater for species with more electronegative substituents (F, Cl, OH) than for the complexes where X = H, CCH and CH₃. Note also the differences in the decomposition for both sub-groups of P...P interactions, in the case of more electronegative substituents the order of the importance of the attractive contributions is CT > POL > ES > XC while for the remaining P...P pnictogen bonds it is POL > CT > ES > XC. The only exception occurs for X = Cl where the polarization energy is the most important attractive term.

The charge transfer energy (CT) correlates very well with the electron density at the P...P BCP, ρ_{PP} , with a linear correlation coefficient, R^2 , of 0.997. There are worse linear correlations between ρ_{PP} and the other attractive term, ES, POL and XC since the linear square correlation coefficient, R^2 , amounts to 0.906, 0.530 and 0.931,

respectively. This means that the characteristics of the BCP, especially the electron density at BCP, reflect mainly the effects connected with the electron charge shift between the interacting units.

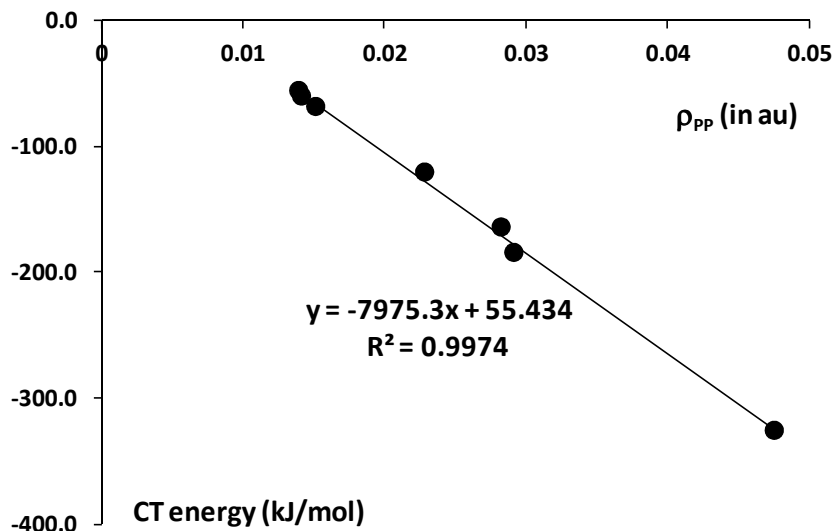


Fig 3. The relationship between the electron density at P...P BCP (in au) and the charge transfer energy (CT) expressed in $\text{kJ}\cdot\text{mol}^{-1}$ units (Eq. 3).

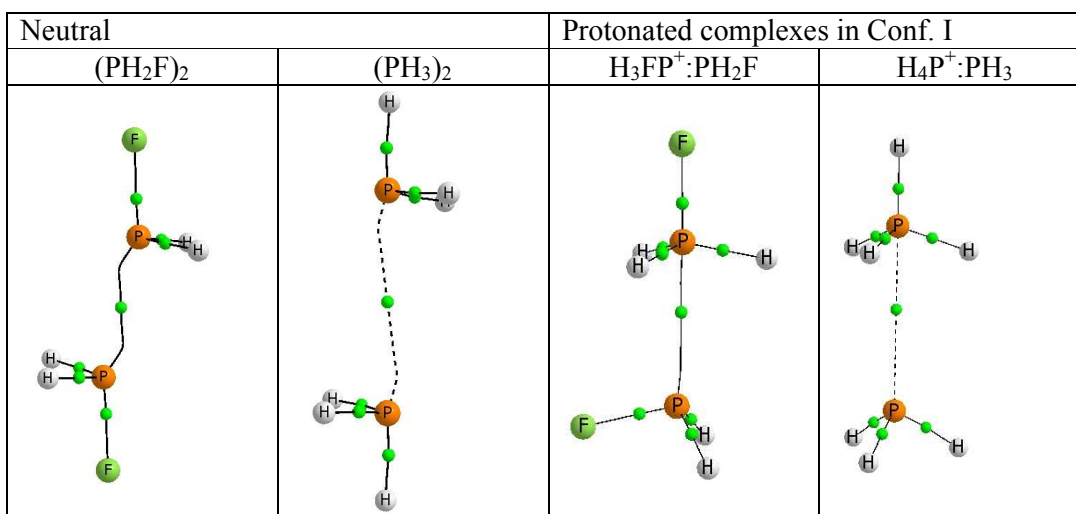
For configuration **II**, presenting a P-H...P hydrogen bond, the order of the importance of the attractive terms is: $\text{CT} > \text{ES} > \text{POL} > \text{XC}$. Thus, the electrostatic contribution for the hydrogen bond is more important than for the P...P interaction. However, this last ranking is based on three configurations where the only intermolecular link is due to the hydrogen bond. For the complexes in configuration **III**, two types of interactions exist, i.e. the P-H...P hydrogen bond and the P...X pnictogen bond, except for the $\text{PH}_3\text{F}^+:\text{PH}_2\text{F}$ complex where only the P...X link exists. In these complexes the energy terms ordering is: $\text{POL} > \text{CT} > \text{ES} > \text{XC}$, the same as for the P...P pnictogen bonds in complexes with CCH, CH_3 and H substituents.

3.5 Comparison of the pnictogen bonded neutral dimers $(\text{PH}_2\text{X})_2$ and protonated binary complexes $\text{PH}_3\text{X}^+:\text{PH}_2\text{X}$ in configuration **I**.

The first difference between these two sets of complexes is the disposition of the groups attached to the interacting phosphorous atoms (Figure 4). In the neutral dimers,

the groups attached to the P atom are pointing outside the interacting region. In contrast, in the protonated complexes the groups of the protonated phosphine points towards the interacting region. Thus, while no direct stereo-electronic interactions between the groups attached in the neutral complexes are expected, the opposite should happen in the protonated complexes.

Figure 4. Molecular graph of two representative neutral complexes and two protonated ones in Conf. I.



The intermolecular P-P distances for the protonated and neutral complexes have been gathered in Table 8. The first interesting feature is that the protonated complexes with $X = \text{F}$, Cl and OH show larger distances than the corresponding neutral ones while for $X = \text{CCH}$, CH_3 and H , the opposite happens. However, a linear correlation is obtained when the distance between the two set of complexes are compared ($R^2 = 0.94$) as indication that the effect of the substituents are similar in both families of complexes.

In order to deepen the analyses of the complexes, some mixed complexes have been considered: the neutral $\text{PH}_3:\text{PH}_2\text{F}$ complex as well as the $\text{PH}_3\text{F}^+:\text{PH}_3$ and $\text{PH}_4^+:\text{PH}_2\text{F}$ ones (Table 8). In the mixed neutral complex, the P-P distance obtained is intermediate of those for the $(\text{PH}_2\text{F})_2$ and $(\text{PH}_3)_2$ dimers an indication that both monomers have similar influence on the characteristic of the complex obtained. In contrast, in the protonated complexes, the intermolecular distance is determined by the protonated phosphine and thus the $\text{PH}_3\text{F}^+:\text{PH}_3$ complex presents a distance similar to the $\text{PH}_3\text{F}^+:\text{PH}_2\text{F}$ one and the $\text{PH}_4^+:\text{PH}_2\text{F}$ complex to the $\text{PH}_4^+:\text{PH}_3$ one.

Table 8. P...P distances (Å) in the protonated complexes in Configuration I and the analogous neutral ones.

Protonated complexes	Conf. I (P...P)	Neutral complexes	(P...P)
PH ₃ F ⁺ :PH ₂ F	2.698	(PH ₂ F) ₂	2.471 ^a
PH ₃ Cl ⁺ :PH ₂ Cl	3.050	(PH ₂ Cl) ₂	2.768 ^a
PH ₃ (OH) ⁺ :PH ₂ (OH) A	2.963	(PH ₂ OH) ₂	2.851 ^a
PH ₃ (OH) ⁺ :PH ₂ (OH) B	2.941		-
PH ₃ (CCH) ⁺ :PH ₂ (CCH)	3.249	(PH ₂ CCH) ₂	3.353 ^a
PH ₃ (CH ₃) ⁺ :PH ₂ (CH ₃)	3.368	(PH ₂ CH ₃) ₂	3.481 ^a
PH ₄ ⁺ :PH ₃	3.356	(PH ₃) ₂	3.589 ^a
PH ₃ F ⁺ :PH ₃	2.718	PH ₃ :PH ₂ F	3.060
PH ₄ ⁺ :PH ₂ F	3.410		

^a taken from ref. 51

The uncorrected binding energies of the protonated and neutral complexes are gathered in Table 9. In all cases, the protonated complexes are more stabilized than their neutral counterparts. The analysis of the mixed complexes, shows that in the neutral case the binding energy is approximately the average of the one of the corresponding neutral dimers while in the protonated ones, the protonated molecule determines the approximate value of the binding energy like in the case of the intermolecular distances.

Table 9. Binding energy (kJ·mol⁻¹) in the protonated complexes in Configuration I and the analogous neutral ones

Protonated complexes	Conf. I		Neutral (PH ₂ X) ₂
PH ₃ F ⁺ :PH ₂ F	-74.9	(PH ₂ F) ₂	-34.0 ^a
PH ₃ Cl ⁺ :PH ₂ Cl	-55.4	(PH ₂ Cl) ₂	-22.1 ^a
PH ₃ (OH) ⁺ :PH ₂ (OH) A	-57.9	(PH ₂ OH) ₂	-20.6 ^a
PH ₃ (OH) ⁺ :PH ₂ (OH) B	-77.1		
PH ₃ (CCH) ⁺ :PH ₂ (CCH)	-55.2	(PH ₂ CCH) ₂	-12.2 ^a
PH ₃ (CH ₃) ⁺ :PH ₂ (CH ₃)	-52.1	(PH ₂ CH ₃) ₂	-8.9 ^a
PH ₄ ⁺ :PH ₃	-46.1	(PH ₃) ₂	-7.1 ^a
PH ₃ F ⁺ :PH ₃	-88.7	PH ₃ :PH ₂ F	-19.2
PH ₄ ⁺ :PH ₂ F	-37.6		

^a taken from ref. 51

The charge transfer and NBO second order energy stabilization of the neutral and protonated complexes have been gathered in Table 10. The neutral (PH₂X)₂ dimers present C_{2h} symmetry and consequently no net charge is transferred from one monomer to the other. In the case of the mixed ones, the binary complex studied here [PH₃:PH₂F],

a small charge transfer is observed from the PH_3 molecule towards the PH_2F . Thus, the latter presents a -0.039 e net charge. In the case of the protonated complexes, an important charge transfer is observed from the neutral molecule towards the protonated one.

Table 10. QTAIM electron charge shift from the Lewis base to the Lewis acid (au) and E_{NBO} orbital charge transfer energies ($\text{kJ}\cdot\text{mol}^{-1}$); the corresponding charge donor orbital- acceptor orbital is listed.

X	Change transfer	E_{NBO}		E_{NBO}
$\text{PH}_3\text{F}^+:\text{PH}_2\text{F}$	0.220	-	$(\text{PH}_2\text{F})_2$	131.8
$\text{PH}_3\text{Cl}^+:\text{PH}_2\text{Cl}$	0.111	33.1	$(\text{PH}_2\text{Cl})_2$	59.9
$\text{PH}_3(\text{OH})^+:\text{PH}_2(\text{OH})$ A	0.163	52.5	$(\text{PH}_2\text{OH})_2$	46.6
$\text{PH}_3(\text{OH})^+:\text{PH}_2(\text{OH})$ B	0.129	48.3		
$\text{PH}_3(\text{CCH})^+:\text{PH}_2(\text{CCH})$	0.075	16.8	$(\text{PH}_2\text{CCH})_2$	11.3
$\text{PH}_3(\text{CH}_3)^+:\text{PH}_2(\text{CH}_3)$	0.070	17.3	$(\text{PH}_2\text{CH}_3)_2$	11.3
$\text{PH}_4^+:\text{PH}_3$	0.067	17.7	$(\text{PH}_3)_2$	5.6

The NBO second order perturbation analysis of the $(\text{PH}_2\text{X})_2$ dimers present two degenerate orbital charge transfer from the lone pair of the P atom of one molecule towards the σ^* P-X of the other or the interaction of the lone pair of one molecule towards the σ -hole of the other.¹¹⁶ In the case of the $\text{PH}_3:\text{PH}_2\text{F}$ binary complex, the two orbital charge transfer are observed but in this case the stabilization due to the PH_3 (lp) $\rightarrow \sigma^*$ P-F is larger than the PH_2F (lp) $\rightarrow \sigma^*$ PH (58.3 vs. 16.5 $\text{kJ}\cdot\text{mol}^{-1}$). In the case of the protonated binary complex, the orbital charge transfer is only from the lone pair of the neutral molecule to the σ^* P-X one. The values of the energy stabilization follow the same trend vs. the P \cdots P interatomic distance as shown in Fig. 5.

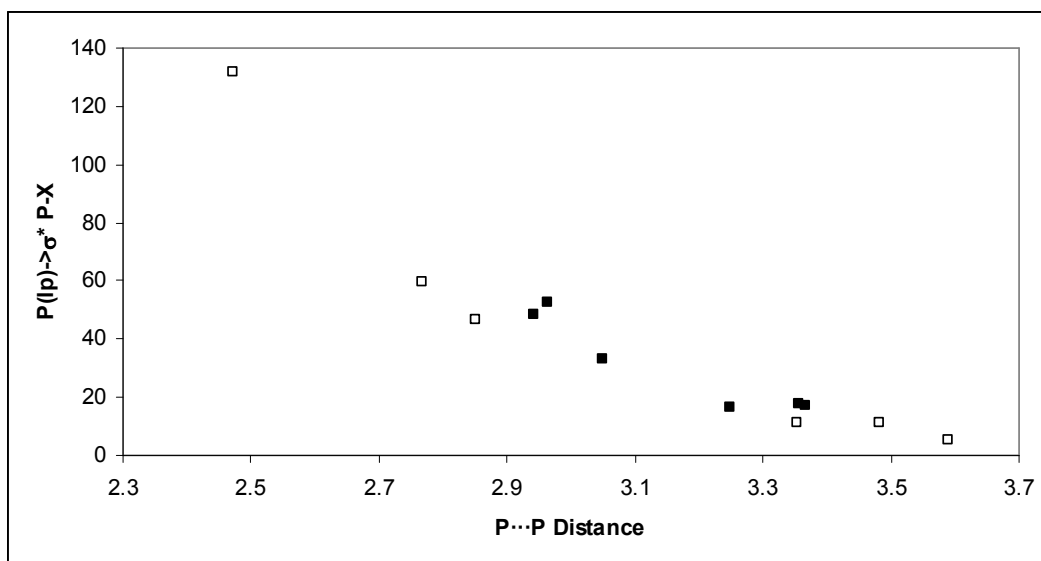


Fig. 5. Energy stabilization due to the charge transfer from the P lone pair towards the P-X σ^* orbital ($\text{kJ}\cdot\text{mol}^{-1}$) vs. the P-P interatomic distance (\AA). Empty and full squares corresponds to the neutral and protonated complexes, respectively.

The topological analysis of the electron density of both neutral and protonated complexes in configuration **I** shows the presence of a bond critical point and its associated bond path linking the two phosphorous atoms (see for instance Fig. 1 and 4). The representation of the values of the electron density at the P-P bond critical point vs. the interatomic distances shows a similar tendency for the values obtained from the neutral or the protonated complexes (Fig. 6).

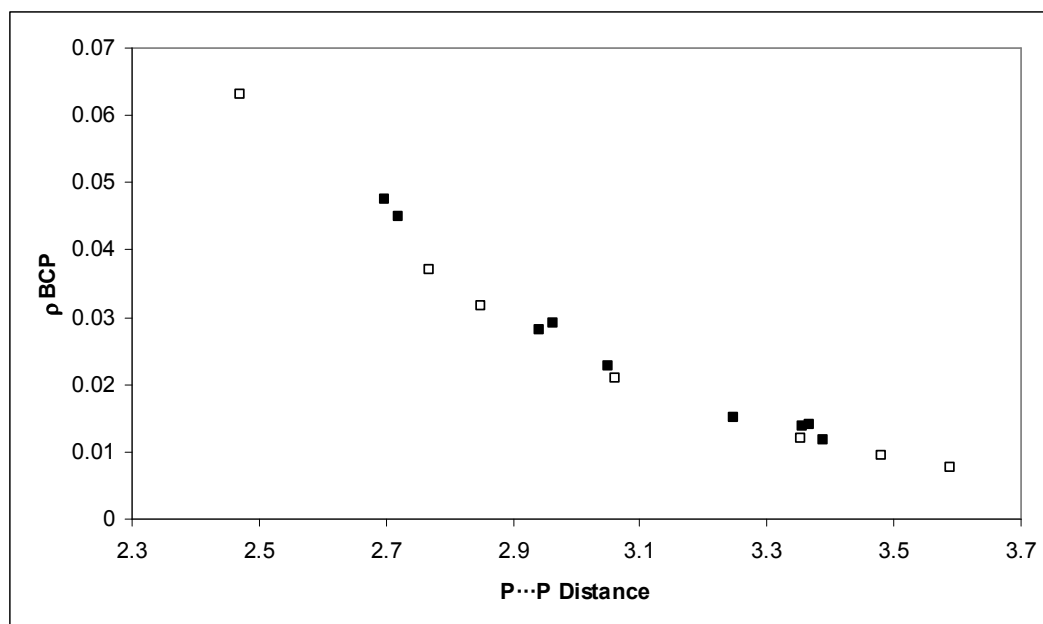


Fig. 6. ρ at the P-P BCP (au) vs. the interatomic distance (Å).

Conclusions

The $\text{PH}_3\text{X}^+:\text{PH}_2\text{X}$ complexes have been analyzed and compared with the $(\text{PH}_2\text{X})_2$ analogues. It was found that the cations are linked through stronger $\text{P}\cdots\text{P}$ pnictogen bonds than the neutral complexes. Thus, positive charge assistance enhances the strength of interaction for pnictogen bonded complexes, similarly as it was found in studies of hydrogen bonded species.⁷¹⁻⁷³

Additionally, for $\text{PH}_3\text{X}^+:\text{PH}_2\text{X}$ complexes, linked through $\text{P}\cdots\text{P}$ or $\text{P}\cdots\text{X}$ pnictogen bonds or through $\text{P}-\text{H}\cdots\text{P}$ hydrogen bonds, different configurations were analyzed. The $\text{P}\cdots\text{P}$ interactions are much stronger than the $\text{P}-\text{H}\cdots\text{P}$ counterparts, and for all species the configurations with $\text{P}\cdots\text{P}$ contacts corresponding to the energetic minima are created while only in few cases there are $\text{P}-\text{H}\cdots\text{P}$ bonded configurations of minimum energy. All energetic, topological and geometrical parameters show that the pnictogen bond is favorable compared with the hydrogen bond for the $\text{PH}_3\text{X}^+:\text{PH}_2\text{X}$ complexes considered here. Even the nature of $\text{P}\cdots\text{P}$ and $\text{P}-\text{H}\cdots\text{P}$ interactions is different. For the previous pnictogen bonds, the order of attractive interaction energy terms is $\text{CT} > \text{PL} > \text{ES}$ and XC , while for $\text{P}-\text{H}\cdots\text{P}$ it is $\text{CT} > \text{ES} > \text{PL}$ and XC . Thus, the electrostatic interaction is a more important attractive term for the hydrogen bond than for the pnictogen bond.

It is also shown here that the characteristics of the P...P bond critical point related to the pnictogen bond correlate with the interaction energy terms, which are usually attributed to the electron charge shift that results of the complexation. This statement is supported, for example, by the linear correlation between the electron density at P...P BCP, ρ_{PP} , and the charge transfer energy as well as by the lack of correlation between the binding energy and ρ_{PP} .

The comparison of the properties of the neutral $(\text{PH}_2\text{X})_2$ and the protonated $\text{PH}_3\text{X}^+:\text{PH}_2\text{X}$ dimers shows some similar features (behaviour of the electronic properties, NBO and AIM, with the P-P distance) but other differences (geometrical disposition, geometric and energetic dependence of the substituents).

Acknowledgments

This work was carried out with financial support from the Spanish Ministerio de Economía y Competitividad (Project No. CTQ2012-35513-C02-02) and Comunidad Autónoma de Madrid (Project FOTOCARBON, ref. S2013/MIT-2841). Financial support comes from Eusko Jaurlaritza (GIC 07/85 IT-330-07) and the Spanish Office for Scientific Research (CTQ2012-38496-C05-04). Technical and human support provided by Informatikako Zerbitzu Orokorra - Servicio General de Informática de la Universidad del País Vasco (SGI/IZO-SGIker UPV/EHU), Ministerio de Ciencia e Innovación (MICINN), Gobierno Vasco Eusko Jaurlanitzza (GV/EJ), European Social Fund (ESF) is gratefully acknowledged.

References

- 1 G. A. Jeffrey and W. Saenger, *Hydrogen Bonding in Biological Structures*, Springer-Verlag: Berlin, 1991.
- 2 G. Zundel, *Hydrogen bonds with large proton polarizability and proton transfer processes in electrochemistry and biology*, in: *Adv. Chem. Phys.* I Prigogine, S. A. Rice, eds. J. Wiley, Vol. 111, 2000.
- 3 J.-M. Lehn, *Angew. Chem. Int. Ed. Engl.* 1990, **29**, 1304–1319.
- 4 J.-M. Lehn, *Supramolecular Chemistry*, Verlag-Chemie, Weinheim, 1995.
- 5 *Hydrogen Bonding – New Insights*, ed. S. J. Grabowski, Vol. 3 of the series: Challenges and Advances in Computational Chemistry and Physics, ed. J. Leszczynski, Springer, 2006.
- 6 H.-J. Schneider, *Angew. Chem. Int. Ed. Engl.*, 2009, **48**, 3924–3977.
- 7 P. Hobza and K. Müller-Dethlefs, *Non-Covalent Interactions, Theory and Experiment*, Royal Society of Chemistry, Cambridge, 2010.
- 8 J. S. Murray, K. E. Riley, P. Politzer and T. Clark, *Aust. J. Chem.*, 2010, **63**, 1598–1607.

- 9 P. Metrangolo and G. Resnati, *Chem. Eur. J.*, 2001, **7**, 2511–2519.
- 10 G. Cavallo, P. Metrangolo, T. Pilati, G. Resnati, M. Sansotera and G. Terraneo, *Chem. Soc. Rev.*, 2010, **39**, 3772–3783.
- 11 L. Wang, J. Gao, F. Bi, B. Song and C. Liu, *J. Phys. Chem. A*, 2014, **118**, 9140–9147.
- 12 P. Metrangolo and G. Resnati, *Halogen Bonding, Struct. Bond.*, 2008, **126**.
- 13 P. Sanz, O. Mó and M. Yáñez, *J. Phys. Chem. A*, 2002, **106**, 4661–4668.
- 14 W. Wang, B. Ji and Y. Zhang, *J. Phys. Chem. A*, 2009, **113**, 8132–8135.
- 15 R. M. Minyaev and V. I. Minkin, *Can. J. Chem.*, 1998, **76**, 776–788.
- 16 M. R. Sundberg, R. Uggla, C. Viñas, F. Teixidor, S. Paavola and R. Kivekäs, *Inorg. Chem. Commun.*, 2007, **10**, 713–716.
- 17 S. Tschirschwitz, P. Lönnecke and E. Hey-Hawkins, *Dalton Trans.*, 2007, 1377–1382.
- 18 J. S. Murray, P. Lane and P. Politzer, *Int. J. Quant. Chem.*, 2007, **107**, 2286–2292.
- 19 S. Bauer, S. Tschirschwitz, P. Lönnecke, R. Franck, B. Kirchner, M. L. Clark and E. Hey-Hawkins, *Eur. J. Inorg. Chem.*, 2009, 2776–2788.
- 20 J. E. Del Bene, I. Alkorta, G. Sánchez-Sanz and J. Elguero, *J. Phys. Chem. A*, 2011, **115**, 13724–13731.
- 21 S. Scheiner, *Chem. Phys. Lett.*, 2011, **514**, 32–35.
- 22 L. Guan, and Y. Mo, *J. Phys. Chem. A*, 2014, **118**, 8911–8921.
- 23 I. Alkorta, I. Rozas and J. Elguero, *J. Phys. Chem. A*, 2001, **105**, 743–749.
- 24 A. Bundhun, P. Ramasami, J. S. Murray and P. Politzer. *J. Mol. Model.*, 2013, **19**, 2739–2746.
- 25 D. Mani and E. Arunan, *Phys. Chem. Chem. Phys.*, 2013, **15**, 14377–14383.
- 26 S. J. Grabowski, *Phys. Chem. Chem. Phys.*, 2014, **16**, 1824–1834.
- 27 A. Bauzá, T. J. Mooibroek and A. Frontera, *Angew. Chem. Int. Ed.*, 2013, **52**, 12317–12321.
- 28 S. A. C. McDowell, *Chem. Phys. Lett.*, 2014, **598**, 1–4.
- 29 Q. Li, X. Guo, X. Yang, W. Li, J. Cheng and H-B. Li, *Phys. Chem. Chem. Phys.*, 2014, **16**, 11617–11625.
- 30 Q.-Z. Li, H.-Y. Zhuo, H.-B. Li, Z.-B. Liu, W.-Z. Li and J.-B. Cheng, *J. Phys. Chem. A*, 2014, in press. DOI: 10.1021/jp503735u
- 31 G. Naray-Szabó and G. G. Ferenczy, *Chem. Rev.*, 1995, **95**, 829–847.
- 32 J. S. Murray and P. Politzer, *Theochem*, 1998, **425**, 107–114.
- 33 R. F. Stewart, *Chem. Phys. Lett.*, 1979, **65**, 335–342.
- 34 *Chemical Applications of Atomic and Molecular Electrostatic Potentials*, ed. P. Politzer and D. G. Truhlar, Plenum Press, New York, 1981.
- 35 T. Clark, M. Hennemann, J. S. Murray and P. Politzer, *J. Mol. Mod.*, 2007, **13**, 291–296.
- 36 J. S. Murray, P. Lane and P. Politzer, *J. Mol. Model.*, 2009, **15**, 723–729.
- 37 P. Politzer, J. S. Murray and T. Clark, *Phys. Chem. Chem. Phys.*, 2010, **12**, 7748–7757.
- 38 P. Politzer and J. S. Murray, *ChemPhysChem.*, 2013, **14**, 278–294.
- 39 P. Politzer, J. S. Murray and T. Clark, *Phys. Chem. Chem. Phys.*, 2013, **15**, 11178–11189.
- 40 S. Zahn, R. Frank, E. Hey-Hawkins and B. Kirchner, *Chem.-Eur. J.*, 2011, **17**, 6034–6038.
- 41 M. Solimannejad, M. Gharabaghi and S. Scheiner, *J. Chem. Phys.*, 2011, **134**, 024312–024316.

-
- 42 S. Scheiner, *J. Chem. Phys.*, 2011, **134**, 094315–094319.
43 S. Scheiner, *J. Phys. Chem. A*, 2011, **115**, 11202–11209.
44 U. Adhikari and S. Scheiner, *J. Phys. Chem. A*, 2012, **116**, 3487–3497.
45 U. Adhikari and S. Scheiner, *Chem. Phys. Lett.*, 2012, **532**, 31–35.
46 S. Scheiner, *Chem. Phys.*, 2011, **387**, 79–84.
47 S. Scheiner, *J. Chem. Phys.*, 2011, **134**, 164313–164319.
48 U. Adhikari and S. Scheiner, *J. Chem. Phys.*, 2011, **135**, 184306–184310.
49 S. Scheiner and U. Adhikari, *J. Phys. Chem. A*, 2011, **115**, 11101–11110.
50 S. Scheiner, *Phys. Chem. Chem. Phys.*, 2011, **13**, 13860–13872.
51 J. E. Del Bene, I. Alkorta, G. Sánchez-Sanz and J. Elguero, *Chem. Phys. Lett.*, 2011, **512**, 184–187.
52 U. Adhikari and S. Scheiner, *Chem. Phys. Lett.*, 2012, **536**, 30–33.
53 Q.-Z. Li, R. Li, X.-F. Liu, W.-Z. Li and J.-B. Cheng, *J. Phys. Chem. A*, 2012, **116**, 2547–2553.
54 Q.-Z. Li, R. Li, X.-F. Liu, W.-Z. Li and J.-B. Cheng, *ChemPhysChem.*, 2012, **13**, 1205–1212.
55 J. E. Del Bene, I. Alkorta, G. Sánchez-Sanz and J. Elguero, *Chem. Phys. Lett.*, 2012, **538**, 14–18.
56 I. Alkorta, G. Sánchez-Sanz, J. Elguero and J. E. Del Bene, *J. Chem. Theor. Comput.*, 2012, **8**, 2320–2327.
57 J. E. Del Bene, I. Alkorta, G. Sánchez-Sanz and J. Elguero, *J. Phys. Chem. A*, 2012, **116**, 9205–9213.
58 S. J. Grabowski, I. Alkorta and J. Elguero, *J. Phys. Chem. A*, 2013, **117**, 3243–3251.
59 P. Politzer, J. S. Murray, G. V. Janjic and S. D. Zaric, *Crystals*, 2014, **4**, 12–31.
60 I. Alkorta, J. Elguero and M. Solimannejad, *J. Phys. Chem. A*, 2014, **118**, 947–953.
61 F. Weinhold and C. Landis, *Valency and Bonding, A Natural Bond Orbital Donor – Acceptor Perspective*, Cambridge University Press 2005.
62 A. E. Reed, L. A. Curtiss and F. Weinhold, *Chem. Rev.*, 1988, **88**, 899–926.
63 R. F. W. Bader, *Atoms in Molecules, A Quantum Theory*; Oxford University Press, Oxford, 1990.
64 P. L. A. Popelier, *Atoms in molecules: An introduction*. Harlow: Prentice Hall, 2000.
65 *Quantum Theory of Atoms in Molecules: Recent Progress in Theory and Application*, ed. C. Matta and R. J. Boyd, Wiley-VCH, 2007.
66 K. Eskandari and N. Mahmoodabadi, *J. Phys. Chem. A* 2013, **117**, 13018–13024.
67 S. Scheiner, *Int. J. Quantum Chem.*, 2013, **113**, 1609–1620.
68 S. Scheiner, *Acc. Chem. Res.*, 2013, **46**, 280–288.
69 S. Grabowski, *Chem. Eur. J.*, 2013, **19**, 14600–14611.
70 S. Grabowski, *ChemPhysChem.*, 2014, **15**, 876–884.
71 P. Gilli, V. Bertolasi, V. Ferretti and G. Gilli, *J. Am. Chem. Soc.*, 1994, **116**, 909–915.
72 G. Gilli and P. Gilli, *J. Mol. Struct.*, 2000, **552**, 1–15.
73 L. Sobczyk, S. J. Grabowski and T. M. Krygowski, *Chem. Rev.*, 2005, **105**, 3513–3560.
74 M. J. Frisch, G. W. Trucks, H. B. Schlegel, G. E. Scuseria, M. A. Robb, J. R. Cheeseman, G. Scalmani, V. Barone, B. Mennucci, G. A. Petersson, H. Nakatsuji, M. Caricato, X. Li, H. P. Hratchian, A. F. Izmaylov, J. Bloino, G. Zheng, J. L.

- Sonnenberg, M. Hada, M. Ehara, K. Toyota, R. Fukuda, J. Hasegawa, M. Ishida, T. Nakajima, Y. Honda, O. Kitao, H. Nakai, T. Vreven, J. A. Montgomery, J. E. Peralta, F. Ogliaro, M. Bearpark, J. J. Heyd, E. Brothers, K. N. Kudin, V. N. Staroverov, R. Kobayashi, J. Normand, K. Raghavachari, A. Rendell, J. C. Burant, S. S. Iyengar, J. Tomasi, M. Cossi, N. Rega, N. J. Millam, M. Klene, J. E. Knox, J. B. Cross, V. Bakken, C. Adamo, J. Jaramillo, R. Gomperts, R. E. Stratmann, O. Yazyev, A. J. Austin, R. Cammi, C. Pomelli, J. W. Ochterski, R. L. Martin, K. Morokuma, V. G. Zakrzewski, G. A. Voth, P. Salvador, J. J. Dannenberg, S. Dapprich, A. D. Daniels, O. Farkas, J. B. Foresman, J. V. Ortiz, J. Cioslowski and D. J. Fox, Gaussian, Inc., Wallingford CT, 2009.
- 75 C. Møller and M. S. Plesset, *Phys. Rev.*, 1934, **46**, 618–622.
- 76 D. E. Woon and T. H. Jr. Dunning, *J. Chem. Phys.*, 1993, **98**, 1358–1371.
- 77 S. F. Boys and F. Bernardi, *Mol. Phys.*, 1970, **19**, 553–566.
- 78 AIMAll (Version 11.08.23), T. A. Keith, TK Gristmill Software, Overland Park KS, USA, 2011 (aim.tkgristmill.com).
- 79 F. Bulat, A. Toro-Labbé, T. Brinck, J. Murray and P. Politzer, *J. Mol. Model.*, 2010, **16**, 1679–1691.
- 80 S. J. Grabowski, *Chem. Rev.*, 2011, **11**, 2597–2625.
- 81 E. D. Glendening and A. Streitwieser, Jr. *J. Chem. Phys.*, 1994, **100**, 2900–2909.
- 82 G. K. Schenter and E. D. Glendening, *J. Phys. Chem.*, 1996, **100**, 17152–17156.
- 83 E. D. Glendening, *J. Am. Chem. Soc.*, 1996, **118**, 2473–2482.
- 84 E. D. Glendening, *J. Phys. Chem A*, 2005, **109**, 11936–11940.
- 85 A. D. Becke, *J. Chem. Phys.*, 1993, **98**, 5648–5652.
- 86 T. H. Dunning, *J. Chem. Phys.*, 1989, **90**, 1007–1023.
- 87 *NBO 5.0*. E. D. Glendening, J. K. Badenhoop, A. E. Reed, J. E. Carpenter, J. A. Bohmann, C. M. Morales and F. Weinhold, Theoretical Chemistry Institute, University of Wisconsin, Madison, 2001.
- 88 M. W. Schmidt, K. K. Baldridge, J. A. Boatz, S. T. Elbert, M. S. Gordon, J. H. Jensen, S. Koseki, N. Matsunaga, K. A. Nguyen, S. J. Su, T. L. Windus, M. Dupuis and J. A. Montgomery, *J. Comput. Chem.*, 1993, **14**, 1347–1363.
- 89 NIST Chemistry WebBook, NIST Standard Reference Database Number 69, eds. P. J. Linstrom and W. G. Mallard.
- 90 I. Alkorta, G. Sánchez-Sanz, J. Elguero and J. E. Del Bene, *J. Phys. Chem. A*, 2014, **118**, 1527–1537.
- 91 L. M. Mentel and E. J. Baerends, *J. Chem. Theory Comput.*, 2014, **10**, 252–267.
- 92 I. Alkorta, C. Trujillo, J. Elguero and M. Solimannejad, *Comput. Theor. Chem.*, 2011, **967**, 147–151.
- 93 J. E. Del Bene, I. Alkorta and J. Elguero, *J. Phys. Chem. A*, 2013, **117**, 6893–6903.
- 94 J.E. Huheey, *J. Phys. Chem.* 1965, **69**, 3284–3291. J.E. Huheey, *J. Phys. Chem.* 1966, **70**, 2086–2092.
- 95 L.C. Allen, *J. Am. Chem. Soc.*, 1989, **111**, 9003–9014.
- 96 R. J. Boyd and S. C. Choi, *Chem. Phys. Lett.*, 1985, **120**, 80–85.
- 97 I. Rozas, I. Alkorta and J. Elguero, *J. Am. Chem. Soc.*, 2000, **122**, 11154–11161.
- 98 O. Knop, K. N. Rankin and R. J. Boyd, *J. Phys. Chem. A*, 2001, **105**, 6552–6566.
- 99 E. Espinosa, I. Alkorta, J. Elguero and E. Molins, *J. Chem. Phys.*, 2002, **117**, 5529–5542.
- 100 T. H. Tang, E. Deretey, S. J. K. Jensen and I. G. Csizmadia, *Eur. Phys. J. D*, 2006, **37**, 217–222.

-
- 101 I. Mata, I. Alkorta, E. Molins and E. Espinosa, *Chem. Eur. J.*, 2010, **16**, 2442–2452.
- 102 R. N. Musin and Y. H. Mariam, *J. Phys. Org. Chem.*, 2006, **19**, 425–444.
- 103 Y. H. Mariam and R. N. Musin, *J. Phys. Chem. A*, 2008, **112**, 134–145.
- 104 D. Cremer and E. Kraka, *Croat. Chem. Acta*, 1984, **57**, 1259–1281.
- 105 S. Jenkins and I. Morrison, *Chem. Phys. Lett.*, 2000, **317**, 97–102.
- 106 W. D. Arnold and E. Oldfield, *J. Am. Chem. Soc.*, 2000, **122**, 12835–12841.
- 107 I. Alkorta, J. Elguero and S. J. Grabowski, *J. Phys. Chem. A*, 2008, **112**, 27121–2727.
- 108 B. Bankiewicz, S. Wojtulewski and S. J. Grabowski, *J. Org. Chem.*, 2010, **75**, 1419–1426.
- 109 R. F. W. Bader, *J. Phys. Chem. A*, 1998, **102**, 7314–7323.
- 110 R. F. W. Bader, *J. Phys. Chem. A*, 2009, **113**, 10391–10396.
- 111 S. J. Grabowski and J. M. Ugalde, *J. Phys. Chem. A*, 2010, **114**, 7223–7229.
- 112 N. Iché-Tarrat, J. C. Barthelat, D. Rinaldi and A. Vigroux, *J. Phys. Chem. B*, 2005, **109**, 22570–22580.
- 113 H. C. Hu and T. Brinck, *J. Phys. Chem. A*, 1999, **103**, 5379–5386.
- 114 T. Clark, *WIREs Comput. Mol. Sci.*, 2013, **3**, 13–20.
- 115 P. Lipkowski and S. J. Grabowski, *Chem. Phys. Lett.*, 2014, **591**, 113–118.
- 116 P. Politzer, J. S. Murray and M. C. Concha, *J. Mol. Model.* 2008, **14**, 659–665